

## Studying the electronic properties of the overlap between (Gallium Arsenic/Titanium Oxide) nanoclusters and (fluorine, Zinc) impurities through DFT

Ahmed Haitham Mezher<sup>\*1a</sup>, Abbas Shwya Alwan<sup>2b</sup> and Vladimir Valentinovich Egorov<sup>3c</sup>

<sup>1</sup>Department of Physics, College of science, University of Thi-Qar, Nasseriya, Iraq.

<sup>2</sup>Department of Physics, College of science, University of Thi-Qar, Nasseriya, Iraq.

<sup>3</sup>Kurchatov Institute, Moscow, Russia.

<sup>b</sup>Email: [abbas.alwan@sci.utq.edu.iq](mailto:abbas.alwan@sci.utq.edu.iq), <sup>c</sup>Email: [egorov@photonics.ru](mailto:egorov@photonics.ru)

<sup>a\*</sup>Corresponding Author: [ahmed.mezher@utq.edu.iq](mailto:ahmed.mezher@utq.edu.iq)

Received: 2025-07-27, Revised: 2025-09-08, Accepted: 2025-11-01, Published: 2025-12-15

**Abstract**— In this study, density functional theory (DFT) calculations have been conducted using the B3LYP hybrid functional with the 6-31G basis set. The computational procedures have been implemented via the Gaussian 09 software package to find out the molecular geometries, electrostatic potential surfaces, contour density maps, infrared spectroscopy (IR) diagnostics, density of states (DOS) schematics, and symmetry of the nanoclusters (4GaAs/2Ti<sub>2</sub>O<sub>3</sub>), (6GaAs/2Ti<sub>2</sub>O<sub>3</sub>), (4GaAs/2Ti<sub>2</sub>O<sub>3</sub>)-4Zn, (4GaAs/2Ti<sub>2</sub>O<sub>3</sub>)-4F, (6GaAs/2Ti<sub>2</sub>O<sub>3</sub>)-4Zn and (6GaAs/2Ti<sub>2</sub>O<sub>3</sub>)-4F. The electronic characteristics: HOMO energy, LUMO energy, band gap ( $E_g$ ), dipole moment, polarizability, electronegativity, and electrophilicity have been evaluated for the nanoclusters under study. The contour density maps revealed the active regions in the molecular system after the overlap between the hybrid nanoclusters (GaAs/Ti<sub>2</sub>O<sub>3</sub>) and the impurities, (fluorine, zinc). One can visualize that the (4GaAs/2Ti<sub>2</sub>O<sub>3</sub>)-4Zn nanocluster exhibited a band gap of approximately to (0.699 eV), which is comparable to that of gallium antimonide (GaSb), which has an energy gap of approximately (0.7 eV), indicating its potential suitability for thermophotovoltaic (TPV) systems, laser diodes, and transistor devices. Furthermore, the symmetry demonstrated that the hybrid nanocluster (4GaAs/2Ti<sub>2</sub>O<sub>3</sub>) has the point group symmetry (Cs/C1), but after the interaction with the impurities, fluorine and zinc, the symmetry becomes (C1). Symmetry merit plays a vital role in optics in physics, especially the optical activity and influence on electronic transition probabilities. The doping by the impurities zinc and fluorine atoms leads to the emergence of new energy states and this is very apparent in the diagrams of the density of states.

**Keywords**— DFT; DOS; infrared spectra; Energy gap; Hybrid nanoclusters.

### I. INTRODUCTION

Nanotechnology is widely regarded as one of the most transformative and rapidly advancing disciplines in modern science. It centers on the manipulation and engineering of matter at the nanometer scale to achieve unprecedented physicochemical properties. These properties, primarily governed by quantum confinement and surface effects, endow nanomaterials with unique behavior that makes them highly advantageous for applications in electronics,

photonics, and catalysis [1]. Among the various nanostructured systems, nanoclusters which typically consist of a few to several hundred atoms have attracted substantial attention due to their size- and composition-dependent properties that deviate markedly from those of their bulk counterparts. These distinctive characteristics include size-tunable optical absorption (e.g., color changes), enhanced catalytic reactivity in noble metals, ductility in otherwise brittle materials, and the emergence of semiconducting or even magnetic behavior in materials that are non-magnetic in bulk form. Additionally, semiconducting nanoclusters may exhibit metallic-like conductivity depending on their structural and compositional features [2]. A critical parameter in determining the behavior of nanoclusters is the HOMO, LUMO energy gap, which is highly sensitive to the cluster's size, elemental composition, and electronic configuration. In this context, hybrid nanoclusters composed of more than one type of material have emerged as particularly promising systems due to their ability to synergistically combine the functionalities of different components. These materials offer broad tenability in electronic and optical properties and have demonstrated potential for advanced applications in nanoelectronics, photovoltaics, and heterogeneous catalysis [3]. Among the key materials in semiconductor research is gallium arsenide (GaAs), a group III–V compound widely utilized in high frequency and optoelectronic devices. GaAs exhibits several favorable characteristics, including a direct band gap, high electron mobility, and excellent thermal stability, making it superior to traditional semiconductors such as silicon and germanium for specific applications [4, 5]. Moreover, doping GaAs introduces discrete energy levels within the band gap, thereby modifying its electrical and optical properties in a controlled manner [6]. On the other hand, titanium oxides, especially nonstoichiometric forms like TiO and Ti<sub>2</sub>O<sub>3</sub>, possess a rich spectrum of electronic phases and structural complexity. These oxides are known for their low cost, chemical and thermal stability, environmental safety, and biocompatibility, alongside their tunable electrical conductivity. Notably, the electrical behavior of titanium oxides strongly depends on the oxygen

stoichiometry:  $\text{Ti}_2\text{O}_3$  in particular can exhibit semiconducting or weakly metallic properties, and it has shown potential for thermoelectric applications [7]. Gallium arsenic can be regarded as one of the most important semiconductors to utilize instead of silicon in the high speed digital electronic circuits and the optoelectronic devices [8]. Titanium oxides or titanium suboxides are obtained incidentally from coal combustion in its abundant environment. The compound  $\text{Ti}_2\text{O}_3$  possesses a superior catalyst efficiency which is attributed to higher surface hydrophilicity [9]. Despite extensive investigations of GaAs and  $\text{Ti}_2\text{O}_3$  as individual materials, studies on hybrid nanoclusters integrating both remain scarce. Furthermore, the effect of doping such hybrid systems with metallic elements such as zinc (Zn) or highly electronegative non-metallic elements such as fluorine (F) on their electronic properties is not yet well understood. Accordingly, the present study aims to theoretically investigate the electronic properties of hybrid GaAs/ $\text{Ti}_2\text{O}_3$  nanoclusters and to evaluate the impact of Zn and F dopants on their electronic structure. Particular attention is given to changes in the HOMO–LUMO gap, charge distribution, and electronic density, with the goal of enhancing the performance of these materials for potential applications in optoelectronics and nanoelectronics.

## II. Computational details

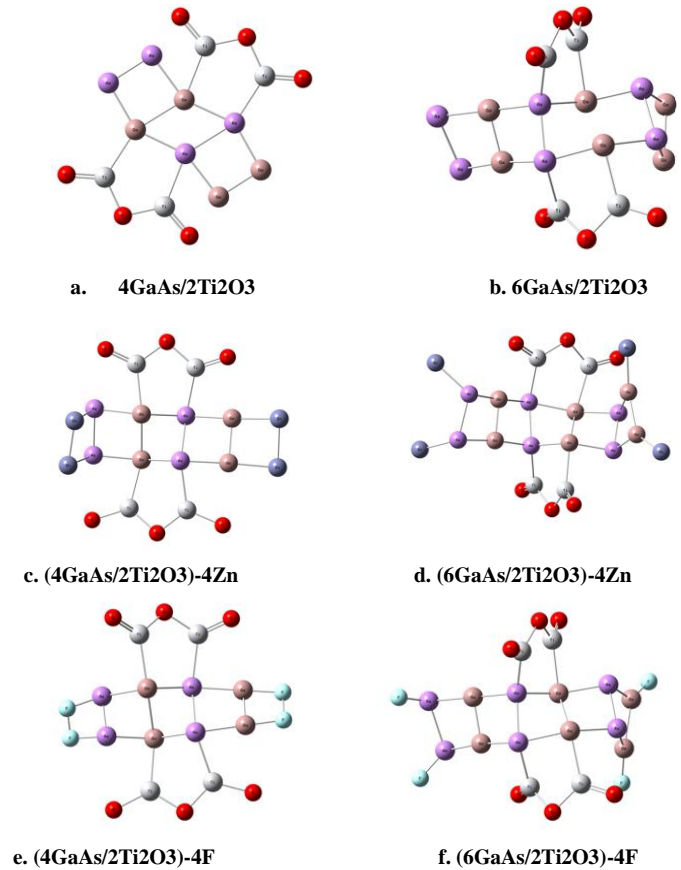
Given the high electronegativity of zinc (Zn) and fluorine (F), both elements exert a significant electronic influence on the core structure of GaAs/ $\text{Ti}_2\text{O}_3$  nanoclusters [10, 11]. To investigate these effects, Zn and F atoms were strategically introduced at the terminal sites of the nanocluster core in two base systems:  $4\text{GaAs}/\text{Ti}_2\text{O}_3$  and  $6\text{GaAs}/\text{Ti}_2\text{O}_3$ . This doping procedure yielded four derivative structures, namely  $4\text{GaAs}/\text{Ti}_2\text{O}_3\cdot 4\text{Zn}$ ,  $4\text{GaAs}/\text{Ti}_2\text{O}_3\cdot 4\text{F}$ ,  $6\text{GaAs}/\text{Ti}_2\text{O}_3\cdot 4\text{Zn}$ , and  $6\text{GaAs}/\text{Ti}_2\text{O}_3\cdot 4\text{F}$ . All structural optimizations, vibrational frequency analyses, and total energy calculations were carried out using the Gaussian 09W software suite [12]. Ground-state electronic properties were computed using the DFT at the B3LYP level of theory, selected for its established reliability in modeling covalent systems, direct heteroatom doping, and nanoscale clusters [13]. The 6-311G(d,p) basis set was employed to ensure a robust description of bonding interactions and lone pair localization [14]. Each optimized structure was verified as a true local minimum by confirming the absence of imaginary vibrational frequencies in the corresponding normal mode analyses [15]. Further insights were obtained using GaussView and GaussSum visualization tools [16, 17], which facilitated the interpretation of optimized geometries, density of states (DOS), infrared (IR) spectra and molecular electrostatic potential (ESP) maps.

## III. RESULTS AND DISCUSSION

### A. Geometrical Structure

The geometrical structure of a molecule or system comprises the spatial configuration of the atoms which consist the molecule or system and it is fundamentally governed by quantum mechanical principles [18]. It

comprises the atoms correlation among them chemically or physically, in which, they seem practically as a one particle. Covalent or ionic bonds, may be originate between the atoms when it approach one another, or it may be no bonding among the atoms. In the case of non-bonding in the geometrical system one can say the system will be non-stable [19]. The molecular structures of the nanoclusters  $4\text{GaAs}/2\text{Ti}_2\text{O}_3$ ,  $6\text{GaAs}/2\text{Ti}_2\text{O}_3$ ,  $(4\text{GaAs}/2\text{Ti}_2\text{O}_3)\cdot 4\text{Zn}$ ,  $(4\text{GaAs}/2\text{Ti}_2\text{O}_3)\cdot 4\text{F}$ ,  $(6\text{GaAs}/2\text{Ti}_2\text{O}_3)\cdot 4\text{Zn}$ ,  $(6\text{GaAs}/2\text{Ti}_2\text{O}_3)\cdot 4\text{F}$  have been accomplished through utilizing the DFT at the ground state, employing the B3LYP hybrid functional and 6-31G basis set by sophisticated algorithms in Gaussian 09 software package.



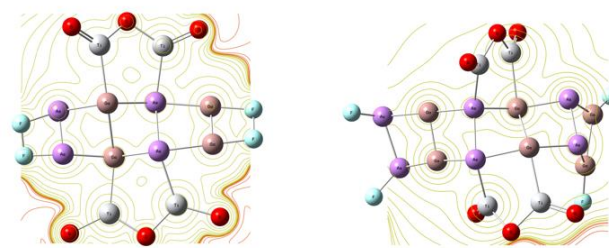
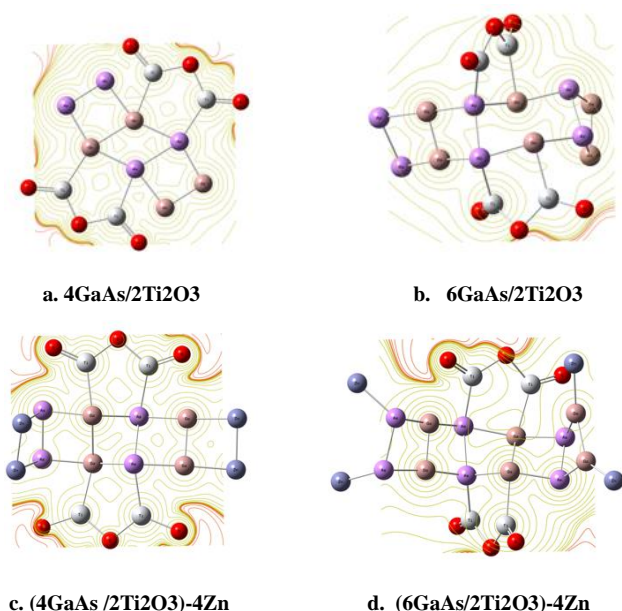
**Fig.1:** The molecular structure of the nanoclusters  $4\text{GaAs}/2\text{Ti}_2\text{O}_3$ ,  $6\text{GaAs}/2\text{Ti}_2\text{O}_3$ ,  $(4\text{GaAs}/2\text{Ti}_2\text{O}_3)\cdot 4\text{Zn}$ ,  $(4\text{GaAs}/2\text{Ti}_2\text{O}_3)\cdot 4\text{F}$ ,  $(6\text{GaAs}/2\text{Ti}_2\text{O}_3)\cdot 4\text{Zn}$  and  $(6\text{GaAs}/2\text{Ti}_2\text{O}_3)\cdot 4\text{F}$ .

Figure (1) demonstrates germanium atoms with light brown color, arsenic atoms with violet color, titanium atoms with light grey color, oxygen atoms with red color, fluorine atoms with light blue color and zinc atoms with light blue color. The molecular structure can be obtained theoretically by using the quintessential programs packages, just like Gaussian 09 or it can be obtained practically in labs. The molecular structure is regarded as a source of information about the chemical and physical properties of the molecules, and it links profoundly with the electronic structure (the distribution of electrons in the orbitals). When the impurities (fluorine and zinc) are close to the hybrid nanoclusters  $(4\text{GaAs}/2\text{Ti}_2\text{O}_3)$  and  $(6\text{GaAs}/2\text{Ti}_2\text{O}_3)$ , there are many physical phenomena may take place, such as charge exchange between the impurities and the hybrid nanoclusters, charge transfer, and adsorption of the atoms of impurities on the surfaces of hybrid nanoclusters.

Gallium arsenic typifies a semiconductor, therefore gallium arsenic trend to make a covalent bonds, also  $\text{Ti}_2\text{O}_3$  is classified as semiconductor and it is trending to make a covalent bonds, fluorine trend to acquire the electrons, zinc is a metal and it trend to donate the electrons, therefore, there is no pure ionic bond will consistence after doping, also there is no pure covalent bond will consistence after doping, hence, may be physics phenomena such as charge exchange occur when the impurities fluorine and zinc close to the surfaces of the hybrid nanoclusters  $(4\text{GaAs}/2\text{Ti}_2\text{O}_3)$  and  $(6\text{GaAs}/2\text{Ti}_2\text{O}_3)$ . In the interaction  $(4\text{GaAs}/2\text{Ti}_2\text{O}_3)$ -4Zn may be the electrons in the outer shell of zinc (two electrons in s orbital) participate the electrons with the electrons in the outer shell of  $(4\text{GaAs}/2\text{Ti}_2\text{O}_3)$ . Also in the interaction  $(4\text{GaAs}/2\text{Ti}_2\text{O}_3)$ -4F may be the electrons in the outer shell of may fluorine participate in electrons with the electrons in the outer shell of  $(4\text{GaAs}/2\text{Ti}_2\text{O}_3)$  through charge exchange between them during the interaction.

### B. Contours

The contour density maps illustrate the spatial distribution of electron charge density around the atoms, also it summarize the active regions in the molecular systems. The regions with crowded contour curves (the active locations) represent the areas of high electron density, it denotes to high concentration of the electronic charges at these regions [20, 21]. The contour maps also help in understanding the overlap mechanism by highlighting on the deformations in the contours that occur through the interaction to consistence the molecular system. The contour density maps of the nanoclusters  $4\text{GaAs}/2\text{Ti}_2\text{O}_3$ ,  $6\text{GaAs}/2\text{Ti}_2\text{O}_3$ ,  $(4\text{GaAs}/2\text{Ti}_2\text{O}_3)$ -4F,  $(6\text{GaAs}/2\text{Ti}_2\text{O}_3)$ -4F,  $(4\text{GaAs}/2\text{Ti}_2\text{O}_3)$ -4Zn, and  $(6\text{GaAs}/2\text{Ti}_2\text{O}_3)$ -4Zn. were achieved by using the DFT, ground-state hybrid function (B3LYP), and basis set (6-31G) during sophisticated algorithms in Gaussian 09 software package.



e.  $(4\text{GaAs}/2\text{Ti}_2\text{O}_3)$ -4F

f.  $(6\text{GaAs}/2\text{Ti}_2\text{O}_3)$ -4F

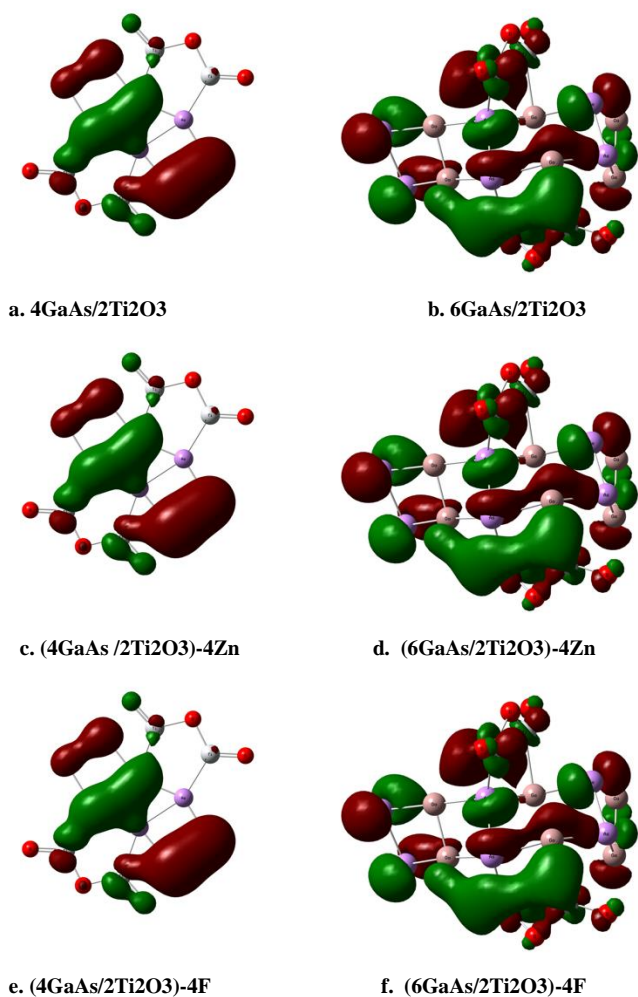
**Fig.2:** The contour density maps of the nanoclusters  $4\text{GaAs}/2\text{Ti}_2\text{O}_3$ ,  $6\text{GaAs}/2\text{Ti}_2\text{O}_3$ ,  $(4\text{GaAs}/2\text{Ti}_2\text{O}_3)$ -4Zn,  $(4\text{GaAs}/2\text{Ti}_2\text{O}_3)$ -4F,  $(6\text{GaAs}/2\text{Ti}_2\text{O}_3)$ -4Zn and  $(6\text{GaAs}/2\text{Ti}_2\text{O}_3)$ -4F.

In Figure (2), the distribution of electron charge density around the atoms and the active regions can be apparently visualized. The distortions in the contour curves (the traffic regions) can be observed in all hybrid nanoclusters, one can visualize that the deformations are being most pronounced near some oxygen atoms. This phenomenon is attributed to the tendency of electrons to remain localized near oxygen atoms, this results as a result to the lowest atomic number of oxygen ( $Z=8$ ) as compared to other atoms in the hybrid nanoclusters, the oxygen atoms own two available orbitals in p to be occupied by the electrons. The orbitals of oxygen atoms be closer to the nuclei, therefore the nucleus attraction force will be stronger in oxygen as compared with the other atoms which consistence the nanoclusters. Also it can be visualized that clear distortions in the contour maps and new active regions are demonstrated distinctly after the overlap, particularly in areas that are adjacent to fluorine and oxygen atoms. This can also be interpreted by the means of the small atomic numbers of the oxygen ( $Z=8$ ) and fluorine ( $Z=9$ ), both of them have p orbitals capable of accepting electrons. This impact is especially prominent in th nanocluster  $(6\text{GaAs}/2\text{Ti}_2\text{O}_3)$ -4F. The analysis of contour maps is considered essential, as it can provide valuable insights into the mechanics of interactions. The contour maps have been employed to express Brillouin zones, Fermi level and Fermi surface in solid-state physics. Many phenomena in solid state physics can be interpret depending of the maps of density contours, just like, physisorption and charge transfer mechanics.

### C. Electrostatic potential (ESP)

Electrostatic potential describes the probability of ability of a molecule or system to perform work as a result of electrostatic interactions. Physically, it represents the scalar value of electrostatic energy that originates between the electronic charges and a point test positive charge; the nucleus set this positive charge [22]. In the Gaussian 09 computational program, the electrostatic potential have been visualized through (HOMO) and (LUMO) surfaces depending on molecular orbital theory, in which the linear combination of the atoms' orbitals gives molecular orbitals [23]. The electrostatic potentials of the nanoclusters  $4\text{GaAs}/2\text{Ti}_2\text{O}_3$ ,  $6\text{GaAs}/2\text{Ti}_2\text{O}_3$ ,  $(4\text{GaAs}/2\text{Ti}_2\text{O}_3)$ -4F,  $(6\text{GaAs}/2\text{Ti}_2\text{O}_3)$ -4F,  $(4\text{GaAs}/2\text{Ti}_2\text{O}_3)$ -4Zn and  $(6\text{GaAs}/2\text{Ti}_2\text{O}_3)$ -4Zn were investigated using the DFT at the ground-state level. The B3LYP functional with the 6-31G basis set was employed for all calculations, which were performed by utilizing of Gaussian 09 software package and GaussView 6.





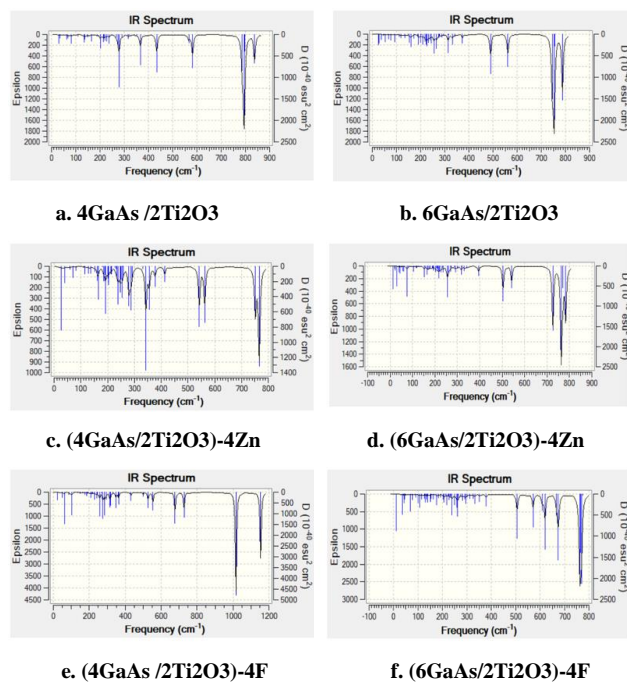
**Fig.3:** The electrostatic potential of the nanoclusters 4GaAs/2Ti<sub>2</sub>O<sub>3</sub>, 6GaAs/2Ti<sub>2</sub>O<sub>3</sub>, (4GaAs/2Ti<sub>2</sub>O<sub>3</sub>)-4Zn, (4GaAs/2Ti<sub>2</sub>O<sub>3</sub>)-4F, (6GaAs/2Ti<sub>2</sub>O<sub>3</sub>)-4Zn and (6GaAs/2Ti<sub>2</sub>O<sub>3</sub>)-4F.

Figure (2), illustrates the distribution of electronic charge density around the atoms of the nanoclusters under study. The charge density is found to be more concentrated in specific regions of the geometrical structure. As a result of the interaction of fluorine atoms with the hybrid nanocluster (4GaAs/2Ti<sub>2</sub>O<sub>3</sub>), one can visualize that the charge density concentrate apparently around some of fluorine atoms, this indicates a strong overlap between those atoms (i.e. fluorine atoms) and the neighboring atoms in the hybrid nanocluster (4GaAs/2Ti<sub>2</sub>O<sub>3</sub>). The interaction between four zinc atoms and the hybrid nanocluster (4GaAs/2Ti<sub>2</sub>O<sub>3</sub>) exhibits charge density distribution clearly around some atoms, but there is no charges distribution around other atoms, which denotes the probability of obtaining shielding procedures. In shielding procedures, the impurities have tendency to interact strongly with some atoms more than the other atoms. Shielding procedure occurs by means of many phenomena, such as, the hybridization, quantum physics constrains and Fermi-Dirac statistic of the distribution of electrons in the molecular system. Another interpretation of shielding procedure in the interaction (4GaAs/2Ti<sub>2</sub>O<sub>3</sub>)-4Zn, these two atoms (the two zinc atoms) set a positive test charges near the surfaces of atoms in order to attract the electronic charges from the hybrid nanocluster (4GaAs/2Ti<sub>2</sub>O<sub>3</sub>), or atoms of the hybrid nanocluster (4GaAs/2Ti<sub>2</sub>O<sub>3</sub>) set a positive test charges near to the surface of nanocluster so as to attract the electrons of those

two atoms (the two zinc atoms). One can visualize the overlap between the hybrid nanocluster (6GaAs/2Ti<sub>2</sub>O<sub>3</sub>) and (fluorine, zinc) lead to charge distribution around all atoms which consistence the nanoclusters, hence, increasing of the molecules of gallium arsenide (GaAs) leads to charge distribution around all atoms of the nanoclusters (6GaAs/2Ti<sub>2</sub>O<sub>3</sub>)-4F and (6GaAs/2Ti<sub>2</sub>O<sub>3</sub>)-4Zn.

#### D. Infrared spectra (IR)

The infrared spectra characterizes the interaction of infrared radiation with the materials. It is expressed during the vibrational modalities. Stretching vibrations are generally classified into symmetric and asymmetric modalities. Symmetric stretching happen when atoms of the same kind vibrate, while, while asymmetric stretching take place when atoms of dissimilar kind oscillate. The harmonic vibrational frequencies can originate within infrared spectroscopy. The vibrational modality be indicated by either domain or bond length [24, 25]. The infrared spectra (IR) of the nanoclusters 4GaAs/2Ti<sub>2</sub>O<sub>3</sub>, 6GaAs/2Ti<sub>2</sub>O<sub>3</sub>, (4GaAs/2Ti<sub>2</sub>O<sub>3</sub>)-4F, (6GaAs/2Ti<sub>2</sub>O<sub>3</sub>)-4F, (4GaAs/2Ti<sub>2</sub>O<sub>3</sub>)-4Zn and (6GaAs/2Ti<sub>2</sub>O<sub>3</sub>)-4Zn were investigated throughout DFT, the hybrid functional B3LYP and 6-31G basis set by utilizing sophisticated algorithms in Gaussian 09 program and Gauss view 06.



**Fig.4:** The infrared spectra of the nanoclusters 4GaAs/2Ti<sub>2</sub>O<sub>3</sub>, 6GaAs/2Ti<sub>2</sub>O<sub>3</sub>, (4GaAs/2Ti<sub>2</sub>O<sub>3</sub>)-4Zn, (4GaAs/2Ti<sub>2</sub>O<sub>3</sub>)-4F, (6GaAs/2Ti<sub>2</sub>O<sub>3</sub>)-4Zn and (6GaAs/2Ti<sub>2</sub>O<sub>3</sub>)-4F.

Figure 4 reveals the formation of new bonds resulting from the interaction of (fluorine, zinc) atoms with the hybrid nanoclusters (4GaAs/2Ti<sub>2</sub>O<sub>3</sub>) and (6GaAs/2Ti<sub>2</sub>O<sub>3</sub>). In the spectrum of (6GaAs/2Ti<sub>2</sub>O<sub>3</sub>)-4F, new active regions are observed at wavenumbers next approximately (1000–1140 cm<sup>-1</sup>), the peaks in this range emerge by the means of the overlap between fluorine atoms with the hybrid nanocluster (6GaAs/2Ti<sub>2</sub>O<sub>3</sub>). The wavenumbers belong to origination bonds of the type (Ga–F), (As–F), (Ti–F), and (O–F). One can visualize that the intensity impact profoundly after the interaction between fluorine atoms and (6GaAs/2Ti<sub>2</sub>O<sub>3</sub>), the highest value of intensity of the hybrid nanocluster (6GaAs/2Ti<sub>2</sub>O<sub>3</sub>) be at (1700 Mole<sup>-1</sup> cm<sup>-1</sup>), while when the

impurities of fluorine adding to the hybrid nanocluster the highest value of intensity is demonstrated at (3500 Mole-1 cm-1) at the wave number (1000 cm-1). The interaction between (4GaAs/2Ti<sub>2</sub>O<sub>3</sub>) and zinc demonstrates comparatively weaker bonds than those formed when (4GaAs/2Ti<sub>2</sub>O<sub>3</sub>) interact with fluorine, one can find out this large dissimilarity in the intensity values on y-axis. The intensity in the nanocluster (4GaAs/2Ti<sub>2</sub>O<sub>3</sub>)-Zn at the wavenumber (750 cm-1) was around (1410 Mole-1 cm-1), but in the nanocluster (4GaAs/2Ti<sub>2</sub>O<sub>3</sub>)-4F the intensity at the same wavenumber becomes more than (2500 Mole-1 cm-1). Hence one can say the bonds (Ga-F), (As-F), (Ti-F), and (O-F) be stronger than the bonds (Ga-Zn), (As-Zn), (Ti-Zn), and (O-Zn), therefore, the fluorine trend to form bonds stronger than zinc.

#### E. Electronic states and energy gap

The energy at the highest occupied molecular orbital is referred to as  $E_{HOMO}$ , while the energy at the lowest unoccupied molecular orbital is referred to as  $E_{LUMO}$ . The energy gap  $E_g$  is considered a critical property in solid-state physics, as it allows for the classification of materials as conductors, insulators, or semiconductors. The width of the energy gap varies depending on the nature of the material: insulators typically exhibit a wide band gap that may exceed 9 eV [26], whereas conductors have no energy gap (i.e., the energy gap must be zero). Mathematically, the energy gap can be expressed by the following equation [27].

$$E_g = E_{LUMO} - E_{HOMO} \dots (1)$$

TABLE I. HOMO ENERGY, LUMO ENERGY, AND ENERGY GAP ( $E_g$ ) OF THE NANOCCLUSERS 4GAAS/2TI<sub>2</sub>O<sub>3</sub>, 6GAAS/2TI<sub>2</sub>O<sub>3</sub>, (4GAAS/2TI<sub>2</sub>O<sub>3</sub>)-4F, (6GAAS/2TI<sub>2</sub>O<sub>3</sub>)-4F, (4GAAS/2TI<sub>2</sub>O<sub>3</sub>)-4ZN AND (6GAAS/2TI<sub>2</sub>O<sub>3</sub>)-4ZN.

System	$E_{LUMO}$ (eV)	$E_{HOMO}$ (eV)	$E_g$ (eV)
4GaAs/2Ti <sub>2</sub> O <sub>3</sub>	-4.3519674	-5.4449931	1.0930257
6GaAs/2Ti <sub>2</sub> O <sub>3</sub>	-4.8779367	-5.6849853	0.8070486
(4GaAs/2Ti <sub>2</sub> O <sub>3</sub> )-4F	-5.232483	-6.1377597	0.9052767
(6GaAs/2Ti <sub>2</sub> O <sub>3</sub> )-4F	-5.4150621	-6.2128593	0.7977972
(4GaAs /2Ti <sub>2</sub> O <sub>3</sub> )-4Zn	-4.2142848	-4.9135818	0.699297
(6GaAs/2Ti <sub>2</sub> O <sub>3</sub> )-4Zn	-4.2997242	-4.9225611	0.6228369

Table (1) shows the energies at the lowest unoccupied molecular orbital (LUMO) and the highest occupied orbital in electron volt (eV). These values are significant according to molecular physics concepts, as they represent the frontier molecular orbitals that play an active role in determining the optical and electronic properties of molecules or systems. When electrons gain energy, they transition from the HOMO level to the LUMO level. The HOMO energy reflects the nanocluster's ability to donate electrons, while the LUMO energy reflects its ability to accept electrons. The energy gap values which are presented in table (1) are within the domain of semiconductor materials, they ranging approximately between approximately (0.62 eV) for (4GaAs/2Ti<sub>2</sub>O<sub>3</sub>)-4Zn and shortly (1.09 eV) for 4GaAs/2Ti<sub>2</sub>O<sub>3</sub>. The energy gap of the nanocluster (4GaAs/2Ti<sub>2</sub>O<sub>3</sub>)-4Zn is remarkably close to that of gallium antimonide (GaSb) energy gap, which has an energy gap be approximately (0.7 eV). This material is particularly important for thermophotovoltaic applications. In general, all values that fall within the energy gap range of semiconductors are considered highly promising for electronic device fabrication, such as microprocessors. The

energy gaps which be close to the value (0.6 eV) are typical of a narrow semiconductor energy gap. One can see in the table the impact of the impurities on the values of energy gap. The impurities fluorine and zinc cause a decrease in the values of the energy gap.

#### F. Point group symmetry

The structure that remains unchanged under rotation by any angle is considered to possess a high degree of symmetry. Accordingly, a sphere exhibits a greater degree of symmetry than a cube, as the latter remains unchanged only at specific rotation angles [28]. Symmetry is a fundamentally important merit in molecular systems, as it enables to the prediction of certain physical characteristics without holding computations [29]. There are seven fundamental symmetry elements: the identity operation ( $E$ ), proper rotation axis ( $C_n$ ), improper rotation axis ( $S_n$ ), inversion center ( $i$ ), horizontal mirror plane ( $\sigma_h$ ), vertical mirror plane ( $\sigma_v$ ), and the dihedral plane ( $\sigma_d$ ) [29, 30].

TABLE II. Summarizes the point group symmetries of the (4GaAs/2Ti<sub>2</sub>O<sub>3</sub>), (6GaAs/2Ti<sub>2</sub>O<sub>3</sub>), (4GaAs/2Ti<sub>2</sub>O<sub>3</sub>)-4F, (6GaAs/2Ti<sub>2</sub>O<sub>3</sub>)-4F, (4GaAs/2Ti<sub>2</sub>O<sub>3</sub>)-4Zn and (6GaAs/2Ti<sub>2</sub>O<sub>3</sub>)-4Zn.

System	Symmetry
4GaAs/2Ti <sub>2</sub> O <sub>3</sub>	$C_s/C_1$
6GaAs/2Ti <sub>2</sub> O <sub>3</sub>	$C_1$
(4GaAs/2Ti <sub>2</sub> O <sub>3</sub> )-4F	$C_1$
(6GaAs/2Ti <sub>2</sub> O <sub>3</sub> )-4F	$C_1$
(4GaAs /2Ti <sub>2</sub> O <sub>3</sub> )-4Zn	$C_1$
(6GaAs/2Ti <sub>2</sub> O <sub>3</sub> )-4Zn	$C_1$

Table (2) summarizes that the interaction between (fluorine , zinc) atoms and 4GaAs/2Ti<sub>2</sub>O<sub>3</sub> in which the nanoclusters (4GaAs/2Ti<sub>2</sub>O<sub>3</sub>)-4F and (4GaAs/2Ti<sub>2</sub>O<sub>3</sub>)-4Zn more symmetric than (4GaAs/2Ti<sub>2</sub>O<sub>3</sub>) because the point group symmetry changes from (Cs/C1) to only C1, The nanoclusters after the overlap, i.e. , (4GaAs/2Ti<sub>2</sub>O<sub>3</sub>)-4F and (4GaAs/2Ti<sub>2</sub>O<sub>3</sub>)-4Zn have the point group symmetry C<sub>n</sub>, in this type of symmetry the system or molecule repeat itself during (2 $\pi$ /n), here, (n=1), therefore these nanoclusters seems the same during the angle (2 $\pi$ ). Studying the symmetry characteristics is very advantageous, as impacts many parameters, such as, the degenerate states, the dipole moment and mechanism of the interaction. Also the molecular structure of the nanoclusters influence pretty much by the symmetry credit. The symmetry property is regarded for treatise the optical properties, just like, the optical activity. The hybrid nanocluster (4GaAs/2Ti<sub>2</sub>O<sub>3</sub>) has the symmetry Cs/C1, The symbol Cs of the point group symmetry means that the procedure stays the molecular structure of the nanocluster same i.e. without any change. Although it is considered of paramount importance theoretically, because it expresses on some processes, as double reflection (reflection followed by reflection) or inversion followed by inversion. By means of possession the nanocluster (4GaAs/2Ti<sub>2</sub>O<sub>3</sub>) the point group symmetry Cs, it possesses two of elements identity a mirror plane. The point group symmetry leave the nanocluster alone, because it possesses the element identity. The point group symmetry Cs is also theoretically significant, as it influences both the electronic and vibrational properties of the system.

## G. Polarizability and Dipole moment

Polarizability is a physical property of a material that describes the ability of a molecule to polarization. Polarizability determines the linear response of the electron density in the presence of an infinite seminal electric field  $F$ , and stands for a second order variation in the energy [31].

$$\alpha = -\left(\frac{\partial^2}{\partial F_a \partial F_b}\right)_{a,b} = x, y, z \quad \dots (2)$$

The polarizability tensors Eigen values  $\alpha_{xx}$ ,  $\alpha_{yy}$  and  $\alpha_{zz}$  are the quantities that determine the value of average polarizability according to the mathematical equation [32].

$$\langle \alpha \rangle = \frac{1}{3}(\alpha_{xx} + \alpha_{yy} + \alpha_{zz}) \quad \dots (3)$$

Dipole moment ( $\mu$ ) is a physical quantity that arises between two charges of equal magnitude but with different signs. Dipole moment generally arises in heteronuclear molecules. The dipole moment is calculated mathematically by equation [33].

$$\mu = q * r \quad \dots (4)$$

TABLE III. Summarizes the average polarizability  $\langle \alpha \rangle$  and dipole moment  $\mu$  values for the nanoclusters (4GaAs/2Ti<sub>2</sub>O<sub>3</sub>), (6GaAs/2Ti<sub>2</sub>O<sub>3</sub>), (4GaAs/2Ti<sub>2</sub>O<sub>3</sub>)-4F, (6GaAs/2Ti<sub>2</sub>O<sub>3</sub>)-4F, (4GaAs/2Ti<sub>2</sub>O<sub>3</sub>)-4Zn, and (6GaAs/2Ti<sub>2</sub>O<sub>3</sub>)-4Zn.

System	$\mu$ (Debye)	$\alpha_{xx}$	$\alpha_{yy}$	$\alpha_{zz}$	$\langle \alpha \rangle$
4GaAs/2Ti <sub>2</sub> O <sub>3</sub>	4.023	737.48	687.2	210.07	544.91
6GaAs/2Ti <sub>2</sub> O <sub>3</sub>	3.06	1029.6	1	752.46	546.98
(4GaAs/2Ti <sub>2</sub> O <sub>3</sub> )-4F	2.53	695.93	673.63	226.65	532.07
(6GaAs/2Ti <sub>2</sub> O <sub>3</sub> )-4F	3.44	930.04	8	740.07	479.93
(4GaAs/2Ti <sub>2</sub> O <sub>3</sub> )-4Zn	8.95	1242.4	9	760.14	312.67
(6GaAs/2Ti <sub>2</sub> O <sub>3</sub> )-4Zn	11.32	2112.8	8	1175.6	818.4

Table (3) shows that the highest polarizability value was observed in the nanocluster (6GaAs/2Ti<sub>2</sub>O<sub>3</sub>)-4Zn, hence the overlap between the zinc atoms and the (6GaAs/2Ti<sub>2</sub>O<sub>3</sub>) nanocluster led to an obvious increase in the average polarizability, it is rising from (544.91 a.u) to (1368.98 a.u). This indicates that the nanocluster (6GaAs/2Ti<sub>2</sub>O<sub>3</sub>)-4Zn typifies the most active nanocluster in the table. The polarizability is of great importance credits for determining the optical properties, such as, the optical basicity, and provides valuable insights into the interatomic structure of materials.

The electric dipole moment is also notably affected by the interaction between zinc atoms and the hybrid nanoclusters. A clear increase is observed, from (4.023 Debye) of the nanocluster (4GaAs/2Ti<sub>2</sub>O<sub>3</sub>) to (8.95 Debye) of the nanocluster (4GaAs/2Ti<sub>2</sub>O<sub>3</sub>)-4Zn. Similarly, the dipole moment increases from (3.06 Debye) in (6GaAs/2Ti<sub>2</sub>O<sub>3</sub>) to (11.32 Debye) in (6GaAs/2Ti<sub>2</sub>O<sub>3</sub>)-4Zn. This makes (6GaAs/2Ti<sub>2</sub>O<sub>3</sub>)-4Zn the nanocluster with the highest dipole moment value among the studied samples in the table. The molecules which that possess a dipole moment are classified as polar, and thus, the dipole moment is a key indicator in distinguishing between polar and

nonpolar bonds. In general, the degree of bond polarity increases with increasing the magnitude of the dipole moment. Studying dipole moments is crucial in the design of optical devices. The nanoclusters with high dipole moments tend to interact strongly with external electric fields or with target molecules, making them highly useful in gas sensors and enhancing electron transport processes.

## H. Electronegativity and Electrophilicity

Electronegativity ( $\chi$ ) is the measurement of an atom's ability to attract a pair of electrons. The first scientist who suggested the idea of electronegativity was Linus Pauling in 1932. Many factors impact to the value of electronegativity such as HOMO energy, LUMO energy, ionization potential, electron affinity and bonding energy. Sometimes the electronegativity is expressed by the chemical potential  $\mu$  Mathematically [30, 34].

$$\mu = \left(\frac{\partial E}{\partial N}\right)_{V(r)} \approx -\chi \quad \dots (5)$$

Also the electronegativity can be expressed in terms of the ionization potential ( $I.P$ ) and electron affinity ( $E.A$ ) as follows [28].

$$\chi = \frac{I.P + E.A}{2} \quad \dots (6)$$

Electrophilicity ( $\omega$ ), sometimes called electron lover, it was first proposed by the scientist (Paar). This is a key property for predicting the reactivity of the system; it also expresses the ability of the atom to accept an additional electron pair to attract the nucleophile, let  $\eta$  typifies the hardness, one can find the electrophilicity from the equation [29].

$$\omega = \frac{\chi^2}{2\eta} \quad \dots (7)$$

TABLE IV. electronegativity and the electrophilicity for the nanoclusters (4GaAs/2Ti<sub>2</sub>O<sub>3</sub>), (6GaAs/2Ti<sub>2</sub>O<sub>3</sub>), (4GaAs/2Ti<sub>2</sub>O<sub>3</sub>)-4F, (6GaAs/2Ti<sub>2</sub>O<sub>3</sub>)-4F, (4GaAs/2Ti<sub>2</sub>O<sub>3</sub>)-4Zn and (6GaAs/2Ti<sub>2</sub>O<sub>3</sub>)-4Zn.

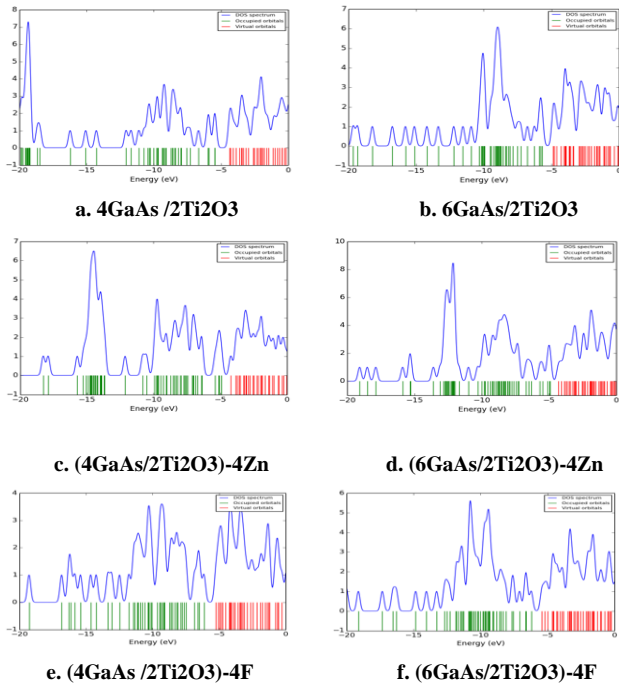
System	$\chi$	$\omega$
4GaAs/2Ti <sub>2</sub> O <sub>3</sub>	4.89848025	21.95292275
6GaAs/2Ti <sub>2</sub> O <sub>3</sub>	5.281461	34.562764
(4GaAs/2Ti <sub>2</sub> O <sub>3</sub> )-4F	5.68512135	35.70245955
(6GaAs/2Ti <sub>2</sub> O <sub>3</sub> )-4F	5.8139607	42.36933775
(4GaAs/2Ti <sub>2</sub> O <sub>3</sub> )-4Zn	4.5639333	29.78632422
(6GaAs/2Ti <sub>2</sub> O <sub>3</sub> )-4Zn	4.61114265	34.13836999

Table (4) demonstrates that the highest value of electronegativity is recorded for the nanocluster (6GaAs/2Ti<sub>2</sub>O<sub>3</sub>)-4F. This indicates that nanocluster (6GaAs/2Ti<sub>2</sub>O<sub>3</sub>)-4F has a greater tendency to form negative ions as compared with the other nanoclusters in the table. Therefore, when the nanocluster (6GaAs/2Ti<sub>2</sub>O<sub>3</sub>)-4F interacts with a molecule of lower electronegativity, the nanocluster (6GaAs/2Ti<sub>2</sub>O<sub>3</sub>)-4F will remove the electrons from it, leading to the formation of bonding force. The electronegativity is a critical parameter, as it not only determines the type of chemical bond formed but also impacts to the direction of bond polarity. It is also affected by the distance between the electrons in the outer shell and the nuclei, where the electrostatic attraction between the electrons and the nuclei decreases as the distance increase.

In addition, table (4) summarizes the values of electrophilicity, which range from shortly (21.95 eV) for the nanocluster (4GaAs/2Ti<sub>2</sub>O<sub>3</sub>) to shortly (42.36 eV) for (6GaAs/2Ti<sub>2</sub>O<sub>3</sub>)-4F. It is visualized that the highest electrophilicity value corresponds to (6GaAs/2Ti<sub>2</sub>O<sub>3</sub>)-4F, making this nanocluster the most reactive among the nanoclusters in the table. Conversely, the nanocluster with the lowest electrophilicity is considered to exhibit the highest stability. The electrophilicity is a crucial property for understanding the chemical behavior of compounds, as it is directly related to the global hardness and softness indices. These indices determine whether the nanocluster behaves as a strong or weak acid, or as a strong or weak base. It can be concluded that the electronic overlap between fluorine and (6GaAs/2Ti<sub>2</sub>O<sub>3</sub>) leads to increase the electrophilicity from (34.56 eV) of the hybrid nanocluster (6GaAs/2Ti<sub>2</sub>O<sub>3</sub>) to the value (42.36 eV) of the nanocluster (6GaAs/2Ti<sub>2</sub>O<sub>3</sub>)-4F.

### I. Density of States (DOS)

The density of states (DOS) stands for the number of allowed states that can be occupied by electrons at specific energy levels, according to quantum mechanics concepts. DOS characteristics are particularly useful in understanding various physical phenomena such as charge transport and charge exchange. It typifies the number of electrons per unit volume within a specific energy domain. In addition, it is essential for determining the number of available states near the energy band edges [35] [36]. The density of states (DOS) of the nanoclusters 4GaAs/2Ti<sub>2</sub>O<sub>3</sub>, 6GaAs/2Ti<sub>2</sub>O<sub>3</sub>, (4GaAs/2Ti<sub>2</sub>O<sub>3</sub>)-4F, (6GaAs/2Ti<sub>2</sub>O<sub>3</sub>)-4F, (4GaAs/2Ti<sub>2</sub>O<sub>3</sub>)-4Zn, and (6GaAs/2Ti<sub>2</sub>O<sub>3</sub>)-4Zn. were achieved by using the DFT, ground-state hybrid function (B3YLP), and basis set (6-31G) during sophisticated algorithms in Gaussian 09 software package with Gauss Sum 03 software.



**Fig.5:** The density of states of the nanoclusters 4GaAs/2Ti<sub>2</sub>O<sub>3</sub>, 6GaAs/2Ti<sub>2</sub>O<sub>3</sub>, (4GaAs/2Ti<sub>2</sub>O<sub>3</sub>)-4Zn, (4GaAs/2Ti<sub>2</sub>O<sub>3</sub>)-4F, (6GaAs/2Ti<sub>2</sub>O<sub>3</sub>)-4Zn and (6GaAs/2Ti<sub>2</sub>O<sub>3</sub>)-4F.

Figure (5) illustrates the relationship between the energy in (eV) and the corresponding allowed states. The density of states (DOS) diagrams are presented for the nanoclusters both before and after adding the impurities. The overlap of the four fluorine atoms with the nanocluster (4GaAs/2Ti<sub>2</sub>O<sub>3</sub>) tends to emergence of new electronic states ~~around~~ between (-20 eV) and (-10 eV), the new states typifies new orbitals that can potentially be occupied by electrons. Similarly, the interaction of the nanocluster (4GaAs/2Ti<sub>2</sub>O<sub>3</sub>) with the four zinc atoms also tends to origination new states between (-20 eV) to (-10 eV), this is indicating to modified energy levels accessed by the electrons occupation. The occupation of these energy levels follows the concepts of quantum physics, Fermi-Dirac statistics and Pauli Exclusion Principle (there is no two electrons may occupy the same quantum state simultaneously). Through the DOS schematics one can know if the material behaves as a conductor, semiconductor or insulator depending on the energy gap between (HOMO) and (LUMO), the energy gap influences by the effective mass of the electrons, the energy gap increase as the effective mass of electron increase. A simplified counter-posing between (4GaAs/2Ti<sub>2</sub>O<sub>3</sub>) and (4GaAs/2Ti<sub>2</sub>O<sub>3</sub>)-Zn depicts that next the energy (-20 eV) the number of states reduces from 7 states to 1 state, this occurs by means of the constrains of the quantum mechanics, in which the electrons can occupy some energetic levels, but it is prohibited to occupy other states.

### III. CONCLUSIONS

This work investigated the electronic and optical properties of hybrid nanoclusters (4GaAs/2Ti<sub>2</sub>O<sub>3</sub> and 6GaAs/2Ti<sub>2</sub>O<sub>3</sub>) doped with Zn and F using DFT. The results demonstrated that Zn and F impurities reduce the energy gap, with the (4GaAs/2Ti<sub>2</sub>O<sub>3</sub>)-4Zn nanocluster reaching ~0.6 eV, close to that of GaSb (0.7 eV), which is promising for thermophotovoltaic (TPV) applications. Charge transfer and charge exchange phenomena were observed through contour maps, ESP distributions, and DOS diagrams, confirming the role of impurities in modifying electronic states. Moreover, the (6GaAs/2Ti<sub>2</sub>O<sub>3</sub>)-4Zn nanocluster exhibited the highest polarizability (1368.98 a.u.) and dipole moment (11.32 Debye), indicating strong potential for optical and dielectric applications, such as capacitors. The (6GaAs/2Ti<sub>2</sub>O<sub>3</sub>)-4F nanocluster showed the maximum electrophilicity, while the pristine (4GaAs/2Ti<sub>2</sub>O<sub>3</sub>) system exhibited the minimum. In particular, the (4GaAs/2Ti<sub>2</sub>O<sub>3</sub>)-4Zn nanocluster demonstrates notable potential for TPV devices. Its energy gap (~0.6 eV) lies within the optimal range for efficient thermal-to-electrical conversion and is comparable to GaSb. This is the fundamental property that makes it promising as a TPV material. Furthermore, Zn doping enhances charge transfer and maintains structural stability, both of which are essential for reliable performance under high-temperature TPV operating conditions. Overall, these findings highlight the tunability of the electronic structure of GaAs/Ti<sub>2</sub>O<sub>3</sub> nanoclusters by Zn and F doping, suggesting promising applications in optoelectronics, thermophotovoltaics, and energy storage devices.



## ACKNOWLEDGMENT

We are deeply appreciative of the provision of essential resources and facilities by University of Thi-Qar, College of Science, and Department of Physics, which facilitated the smooth execution of our research activities. This research is a part of the Master graduation requirements.

## CONFLICT OF INTEREST

Authors declare that they have no conflict of interest.

## REFERENCES

- [1] M. Negahdary and S. Mabbott, "Automated synthesis and processing of functional nanomaterials: Advances and perspectives," *Coordination Chemistry Reviews* vol. 523, p. 216249, 2025.
- [2] M. Galchenko, A. Black, L. Heymann, and C. Klinke, "Field effect and photoconduction in Au<sub>25</sub> nanoclusters films," *Advanced Materials* vol. 31, no. 18, p. 1900684, 2019.
- [3] N. A. Besley, R. L. Johnston, A. J. Stace, and J. Uppenbrink, "Theoretical study of the structures and stabilities of iron clusters," *Journal of Molecular Structure: THEOCHEM* vol. 341, no. 1-3, pp. 75-90, 1995.
- [4] F. Smith *et al.*, "Picosecond GaAs-based photoconductive optoelectronic detectors," in *Picosecond Electronics and Optoelectronics*, 1989, p. OSDA176: Optica Publishing Group.
- [5] F. Smith, A. Calawa, C.-L. Chen, M. Manfra, and L. Mahoney, "New MBE buffer used to eliminate backgating in GaAs MESFETs," *IEEE Electron Device Letters* vol. 9, no. 2, pp. 77-80, 1988.
- [6] M. C. Esteves, A. B. Rocha, N. V. Vugman, and C. E. Bielschowsky, "DFT calculation of EPR parameters of antisite defect in gallium arsenide," *Chemical Physics Letters* vol. 453, no. 4-6, pp. 188-191, 2008.
- [7] A. A. Valeeva, S. Z. Nazarova, and A. A. Rempel, "Nanosize effect on phase transformations of titanium oxide Ti<sub>2</sub>O<sub>3</sub>," *J Journal of Alloys Compounds* vol. 817, p. 153215, 2020.
- [8] T. Oxley and C. Corbey, "Systems applications of GaAs devices and ICs," *Microprocessors Microsystems* vol. 11, no. 8, pp. 443-449, 1987.
- [9] X. Pei, T. Zhang, J. Zhong, Z. Chen, C. Jiang, and W. Chen, "Substoichiometric titanium oxide Ti<sub>2</sub>O<sub>3</sub> exhibits greater efficiency in enhancing hydrolysis of 1, 1, 2, 2-tetrachloroethane than TiO<sub>2</sub> nanomaterials," *Science of The Total Environment* vol. 774, p. 145705, 2021.
- [10] J. Huo *et al.*, "Synthesis of F-doped materials and applications in catalysis and rechargeable batteries," *Nanoscale Advances*, vol. 5, no. 11, pp. 2846-2864, 2023.
- [11] H. Zeng, M. Wu, M. Cheng, and Q. Lin, "Effects of Cu, Zn doping on the structural, electronic, and optical properties of  $\alpha$ -Ga<sub>2</sub>O<sub>3</sub>: first-principles calculations," *Materials* vol. 16, no. 15, p. 5317, 2023.
- [12] M. Frisch, "gaussian 09, Revision d. 01, Gaussian," *Inc, Wallingford CT*, vol. 201, 2009.
- [13] I. Y. Zhang, J. Wu, and X. Xu, "Extending the reliability and applicability of B3LYP," *Chemical Communications*, vol. 46, no. 18, pp. 3057-3070, 2010.
- [14] F. Hassan, B. Daraam, and A. Shwya, "Density Functional Theory Investigation for Sodium Atom on Copper Clusters," ed: IJSR, 2015.
- [15] F. Jensen, *Introduction to computational chemistry*. John Wiley & sons, 2017.
- [16] R. Dennington, T. Keith, J. Millam, and V. GaussView, "Semichem Inc," *Shawnee Mission KS, GaussView, Version* vol. 5, no. 8, 2009.
- [17] N. M. O'boyle, A. L. Tenderholt, and K. M. Langner, "Cclib: a library for package-independent computational chemistry algorithms," *Journal of computational chemistry* vol. 29, no. 5, pp. 839-845, 2008.
- [18] A. S. Alwan, "Density functional theory investigation of (C<sub>4</sub>H<sub>2</sub>N<sub>2</sub>)<sub>3</sub> nanocluster and (C<sub>4</sub>H<sub>2</sub>N<sub>2</sub>)<sub>3</sub>--P, Al, As, B, C and in nanoclusters," in *AIP Conference Proceedings*, 2020, vol. 2292, no. 1, p. 030013: AIP Publishing LLC.
- [19] R. DeKock and H. Gray, "Chemical Bonding and Structure," ed: Benjamin/Cummings Publishing Inc. Menlo Park, CA, 1980.
- [20] S. H. Talib and A. S. Alwan, "Geometrical Optimization and Some Electronical Properties for Pyrrole-Metal Interactions Using DFT, B3LYP Basis Sets," *Journal of Optoelectronics Laser* vol. 41, no. 7, pp. 1300-1312, 2022.
- [21] A. B. Ahmed, "Studying the electronic characteristics and physisorption of OTS on the pure silver surfaces (Ag<sub>10</sub>), (Ag<sub>15</sub>) and (Ag<sub>18</sub>)," *University of Thi-Qar Journal of Science* vol. 10, no. 2, pp. 151-159, 2023.
- [22] J. A. Bristol and A. M. Doherty, *Annual reports in medicinal chemistry*. Academic Press, 1998.
- [23] M. Frisch, "gaussian 09, Revision d. 01, Gaussian," *Inc, Wallingford CT*, vol. 201, 2009.
- [24] K. Sadasivam and R. Kumaresan, "Theoretical investigation on the antioxidant behavior of chrysoeriol and hispidulin flavonoid compounds—A DFT study," *Computational Theoretical Chemistry*, vol. 963, no. 1, pp. 227-235, 2011.
- [25] P. Gupta, S. S. Das, and N. Singh, *Spectroscopy*. Jenny Stanford Publishing, 2023.
- [26] A. Forouhi and I. Bloomer, "New dispersion equations for insulators and semiconductors valid throughout radio-waves to extreme ultraviolet spectral range," *Journal of Physics Communications*, vol. 3, no. 3, p. 035022, 2019.
- [27] S. M. Sze, *Semiconductor devices: physics and technology*. John Wiley & sons, 2008.
- [28] M. L. Jabbar, "Theoretical study for the interactions of Coronene-Y interactions by using Density functional theory with hybrid function," *University of Thi-Qar Journal* vol. 13, no. 3, pp. 28-41, 2018.
- [29] A. M. Lesk, *Introduction to symmetry and group theory for chemists*. Springer, 2004.



- [30] D. C. Harris and M. D. Bertolucci, *Symmetry and spectroscopy: an introduction to vibrational and electronic spectroscopy*. Courier Corporation, 1989.
- [31] J. P. Inchaustegui and R. Pumachagua, "Computational study on second-order nonlinear optical properties of donor-acceptor substituted copper phthalocyanines," *Revista de la Sociedad Química del Perú* vol. 81, no. 3, pp. 232-241, 2015.
- [32] A. M. Ali, "Investigations of some antioxidant materials by using density functional and semiempirical theories," *P. hD. Thesis, Univ. Basrah, Coll. Sci. Dep. Phys* 2009.
- [33] M. K. Hommod and L. F. Auqla, "Density Functional Theory Investigation For Ni6, Co5, Au12, Y5 and Ni6Li, Co5Li, Au12Li, Y5Na Interactions," *University of Thi-Qar Journal of Science* vol. 9, no. 2, pp. 105-112, 2022.
- [34] A. S. Alwan and S. H. Talib, "Quantum Computational Study of the electronic properties of the interactions between 3THF and Some Metallic Linear Molecules Using DFT," *Journal of Education for Pure Science* vol. 11, no. 2, pp. 53-67, 2021.
- [35] C. Kittel and P. McEuen, *Introduction to solid state physics*. John Wiley & Sons, 2018.
- [36] M. A. Omar, *Elementary solid state physics: principles and applications*. Pearson Education India, 1999.